JOURNAL OF THERMOPHYSICS AND HEAT TRANSFER
Vol. 9, No. 1, January–March 1995

Heat Transfer Variation on Protuberances and Surface Roughness Elements

Robert C. Henry*
ONERA, 92322 Chatillon Cedex, France
and
R. John Hansman Jr.† and Kenneth S. Breuer‡
Massachusetts Institute of Technology, Cambridge, Massachusetts 02139

In order to determine the effect of surface irregularities on local convective heat transfer, the variation in heat transfer coefficients on small (2–6 mm diam) hemispherical roughness elements on a flat plate has been studied in a wind tunnel using IR techniques. Heat transfer enhancement was observed to vary over the roughness elements with the maximum heat transfer on the upstream face. This heat transfer enhancement increased strongly with roughness size and velocity when there was a laminar boundary layer on the plate. For a turbulent boundary layer, the heat transfer enhancement was relatively constant with velocity, but did increase with element size. When multiple roughness elements were studied, no influence of adjacent roughness elements on heat transfer was observed if the roughness separation was greater than approximately one roughness element radius. As roughness separation was reduced, less variation in heat transfer was observed on the downstream elements. Implications of the observed roughness enhanced heat transfer on ice accretion modeling are discussed.

I. Introduction

UNDERSTANDING the detailed structure of the convective heat transfer on irregular ice surfaces is central to successfully modeling aircraft ice accretion, particularly in the wet "glaze" ice growth regime. In glaze icing, the accretion is controlled by the rate at which latent heat can be convected away from the icing surface.[1] Recent close-up video studies have observed enhanced "feather" ice growth from the upstream face of surface roughness elements.[2] An example of feather growth is shown in Fig. 1. Feather growth is thought to be initiated by local enhancement in heat transfer that occurs on surface roughness elements.

Most prior studies of convective heat transfer from roughened surfaces have focused on cases where the roughness element height was small compared with the boundary-layer thickness,[3,4] or on cases where the large fins or protuberances extend through the boundary layer.[5–7] In addition, most traditional heat transfer experimental methods investigate the heat transfer averaged over many roughness elements.[8] Because local variation of heat transfer on the scale of the roughness elements size appears to be important to feather growth initiation in ice accretion, it was necessary to develop experimental techniques to study heat transfer at high spatial resolution.

II. Experimental Approach

The experimental approach was to investigate the local perturbations in heat transfer caused by roughness elements through thermographic studies of a uniformly heated surface. When the surface is heated, the steady-state surface temperature can be related to the convective heat transfer coefficient.

The method is shown schematically in Fig. 2. In steady state, Q_{in} from external heating is balanced by the sum of heat losses. These include: convective flux Q_{conv}, conductive flux into the plate Q_{cond}, and radiative flux Q_{rad}:

$$Q_{in} = Q_{out} = Q_{conv} + Q_{cond} + Q_{rad} \tag{1}$$

If the surface is composed of a material with low thermal conductivity, the heat conduction losses Q_{cond} can be assumed to be small in steady state. Radiative losses are typically less than 1% of the convective losses for room temperature, wind-tunnel experiments, and can also be neglected. Under these assumptions, the primary heat sink for the surface is convective flux, which can be written as

$$Q_{conv} = h(T_{sur} - T_0) \tag{2}$$

where h is the convective heat transfer coefficient, T_{sur} is the surface temperature, and T_0 is the freestream temperature.

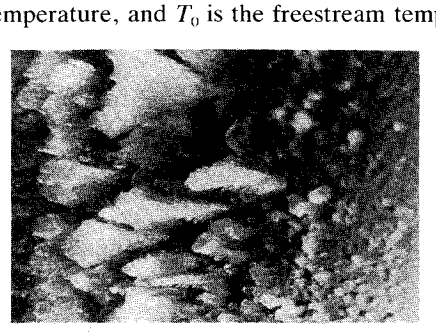

Fig. 1 Example of feather ice growth.

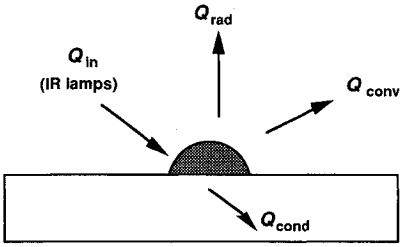

Fig. 2 Energy balance on a roughness element.

Received Sept. 28, 1993; presented as Paper 94-0801 at the AIAA 32nd Aerospace Sciences Meeting, Reno, NV, Jan. 10–13, 1994; revision received May 9, 1994; accepted for publication May 11, 1994.

*Research Engineer, Physics Department. Member AIAA.
†Associate Professor, Department of Aeronautics and Astronautics. Member AIAA.
‡Assistant Professor, Department of Aeronautics and Astronautics. Member AIAA.

Since $Q_{in} = Q_{conv}$, the convective heat transfer coefficient can be written as

$$h = [Q_{in}/(T_{sur} - T_0)] \tag{3}$$

If the heating is relatively uniform (i.e., Q_{in} is constant), the convective heat transfer coefficient in the area perturbed by the roughness elements h_p, normalized by convective heat transfer coefficient in the uniform unperturbed area just upstream of the roughness element h_u, can be related to the surface temperatures in the perturbed and unperturbed regions:

$$\frac{h_p}{h_u} = \frac{(T_{sur_u} - T_0)}{(T_{sur_p} - T_0)} \tag{4}$$

The surface temperatures can be measured with an IR camera, and the freestream temperature can be measured by thermocouples. This allows a noninvasive measurement of the local heat transfer enhancement limited only by the spatial resolution of the IR camera.

III. Experimental Setup

Heat transfer measurements were performed in a low-turbulence (less than 0.2%), 1- × 1-ft (30.5- × 30.5-cm) wind tunnel,[9] using the experimental setup shown in Fig. 3. The test roughness elements were mounted on a 50-cm-long, 30-cm-wide flat Plexiglas® plate, and were observed with an IR camera.

Test roughness elements typically consisted of plastic hemispherical beads. The test location was in the center of the plate, 25 cm downstream from the leading edge. The plate had a beveled leading edge with a 1.5-mm nose radius. The plate was observed by IR imaging techniques to have uniformly high surface temperatures, indicating a laminar boundary layer at the test location, for Reynolds numbers less than 3×10^5. For turbulent boundary-layer tests, a 0.5-mm-diam wire was placed at the leading edge of the plate to trip the boundary layer. The turbulent boundary layer was verified by a drop in plate surface temperature (typically greater than 10°F) with the trip wire present. Thermocouples were included in the experimental setup to provide freestream air temperature data and reference surface temperature readings.

The test surface was heated with three IR lamps to provide uniform heating in the roughness element area. Uniformity of heating was verified by measuring surface temperature without external flow. The plate and roughness elements were painted flat black to aid in uniform heating and to avoid false IR temperature signals due to heat reflection.

A Hughes Probeye thermal video system was used to map surface temperatures. The IR camera was located above the plate and was focused on the roughness element zone through a hole in the upper wall of the test section. Spatial resolution was smaller than 1 mm, and temperature resolution was approximately 1°F. The IR system displayed a color video image with temperature scales and temperature plots on selected cross sections. Temperature range and sensitivity could be adjusted and surface emissivity could be compensated for. Due to the flat black surface, emissivity was assumed to be equal to unity and a high-temperature sensitivity between 0.8–1°F was generally used. The IR images were recorded on a VCR for subsequent analysis.

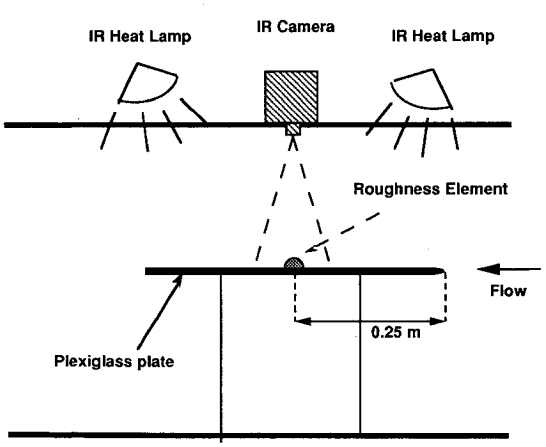

Fig. 3 Schematic view of the experimental setup.

IV. Test Procedure

Tests were performed for freestream velocities varying from 5 to 31 m/s, resulting in Reynolds numbers from 1×10^5 to 5×10^5 at a test location 25-cm downstream from the leading edge. For each test, IR thermographs of the roughness element region were recorded, and the relative heat transfer coefficient was calculated vs position in the flow direction.

Three series of tests were performed with laminar and/or turbulent boundary layers. The first investigated the effect of roughness element size for single elements. The second investigated the effect of interaction between multiple roughness elements. The third focused on the effect of arrangement and packing density for multiple roughness elements.

V. Relative Heat Transfer Coefficient Accuracy

For low-speed tests (5 m/s), typical values of $(T_{sur} - T_0)$ were on the order of 30°F (17°C) in the unperturbed region, and 20°F (11°C) in the perturbed region. Assuming uncertainty in surface temperature measurement of 1°F, this would correspond to an uncertainty of heat transfer coefficient ratio of approximately 8%. For high-speed tests (31 m/s), $(T_{sur} - T_0)$ values were typically 15°F (9°C) in the unperturbed region, and 7°F (4°C) in the perturbed region, corresponding to an uncertainty of 20%.

VI. Experimental Results

A. Individual Roughness Element Effects

In order to investigate heat transfer on individual roughness elements, the configuration shown in Fig. 4 was tested. The configuration consisted of four spherical roughness elements with heights varying from 0.75 to 2.8 mm. It should be noted that the elements were slightly shorter than full hemispheres. Consequently, the base radii were larger than the heights. The center of each element was located 25 cm downstream from the plate leading edge, and the cross-stream separation between each element was approximately 3 mm. This configuration was tested with both laminar and turbulent boundary layers.

B. Laminar Boundary-Layer Results

1. Typical Infrared Image

A typical IR thermograph of three elements (2.8, 0.7, and 1.7 mm high) at a freestream velocity of 22 m/s is shown in Fig. 5. The flow is from the right, and gray shades indicate

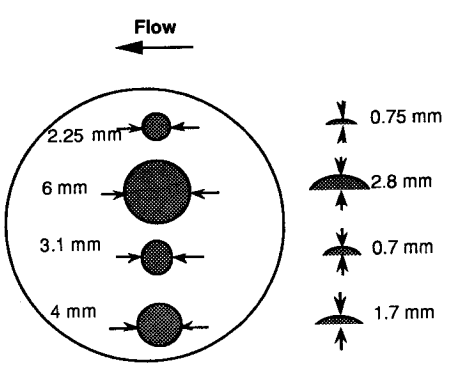

Fig. 4 Individual roughness element test configuration.

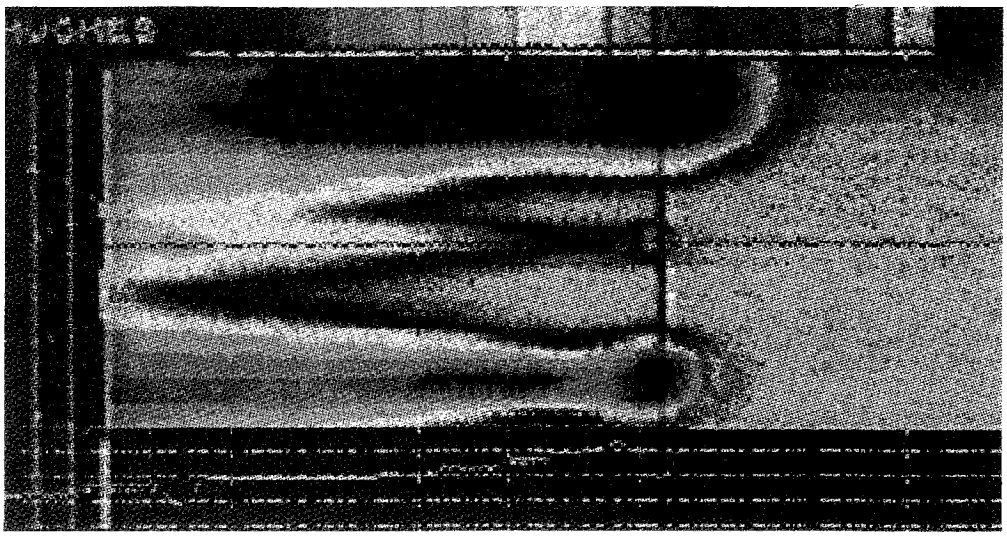

Fig. 5 Infrared thermograph of 2.8-, 0.7-, and 1.7-mm-high roughness elements in a laminar boundary layer. Note the uniform temperature in the unperturbed region upstream (to the right) of the elements.

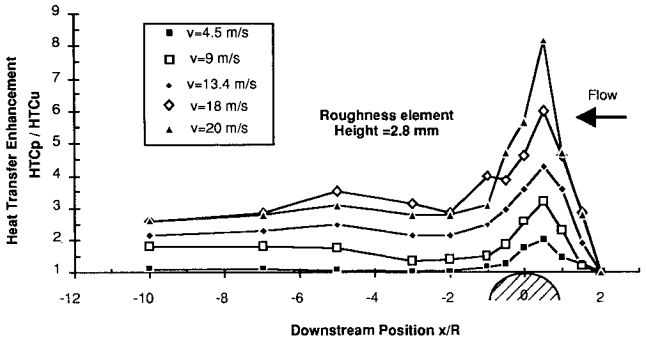

Fig. 6 Heat transfer coefficient enhancement profile on a 2.8-mm-high roughness element in a laminar boundary layer.

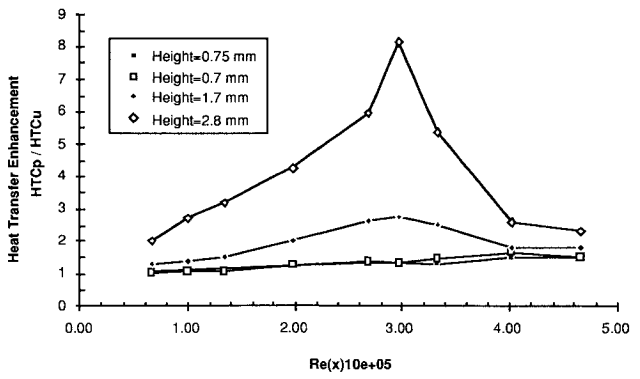

Fig. 7 Maximum heat transfer coefficient enhancement in a laminar boundary layer vs Reynolds number 25 cm downstream of the plate leading edge.

temperature contours in the thermographic image. Significant variation in surface temperature and hence, heat transfer, can be seen on each roughness element with the coldest regions (i.e., highest heat transfer) on the upstream side of the elements. A second cold region is also observed in the boundary-layer transition wedge downstream of the elements. The 2.8- and 1.7-mm-high elements are seen to be significantly colder than the 0.7-mm-high element.

2. Heat Transfer Enhancement Profiles

The heat transfer enhancement profiles for the 2.8-mm-high roughness element are plotted in Fig. 6 for several velocities. The profiles are taken through the middle of the element and downstream distance is normalized by the radius of the bead (3 mm). The general shape of the curves are the same for each velocity. The heat transfer begins to increase at a distance of approximately 2-radii upstream of the elements. A peak in heat transfer is observed on the upstream face at about one-half radius downstream the leading edge of the bead. Then, the heat transfer coefficient decreases sharply to the downstream edge of the element. The heat transfer enhancement in the wake is typically 50% of the maximum value. Similar profiles were found for other roughness element sizes.

3. Maximum Heat Transfer Enhancement

The peak of heat transfer value, corresponding to the coldest region, was found to be located approximately one-half radius downstream the leading edge of the bead. This maximum heat transfer coefficient enhancement is plotted in Fig. 7 as a function of the Reynolds number for the different roughness elements tested.

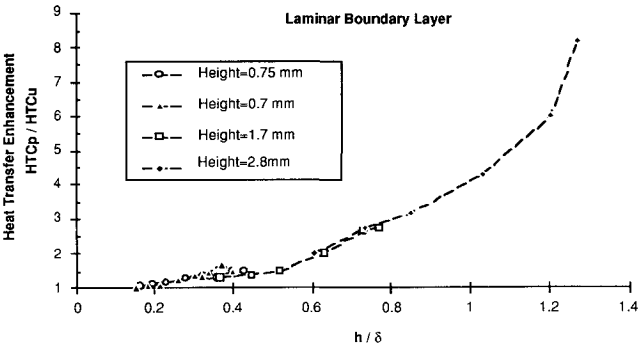

Fig. 8 Maximum heat transfer coefficient enhancement vs ratio of height of element to the theoretical laminar boundary-layer thickness.

For the small roughness elements, the heat transfer enhancement is observed to be small and weakly dependent on Reynolds number in the range tested. For the larger elements, the enhancement is larger and is seen to increase with Reynolds number until a maximum at $Re = 3 \times 10^5$. Above this value the boundary layer is assumed to have transitioned to turbulent. And the decreased enhancement is due to increased heat transfer in the unperturbed region.

The heat transfer coefficient maximum increase is plotted vs the ratio of roughness element height to the theoretical boundary-layer thickness δ, obtained from Schlichting[10] for the laminar cases in Fig. 8. When the element height is smaller than the half of the theoretical boundary-layer thickness, heat

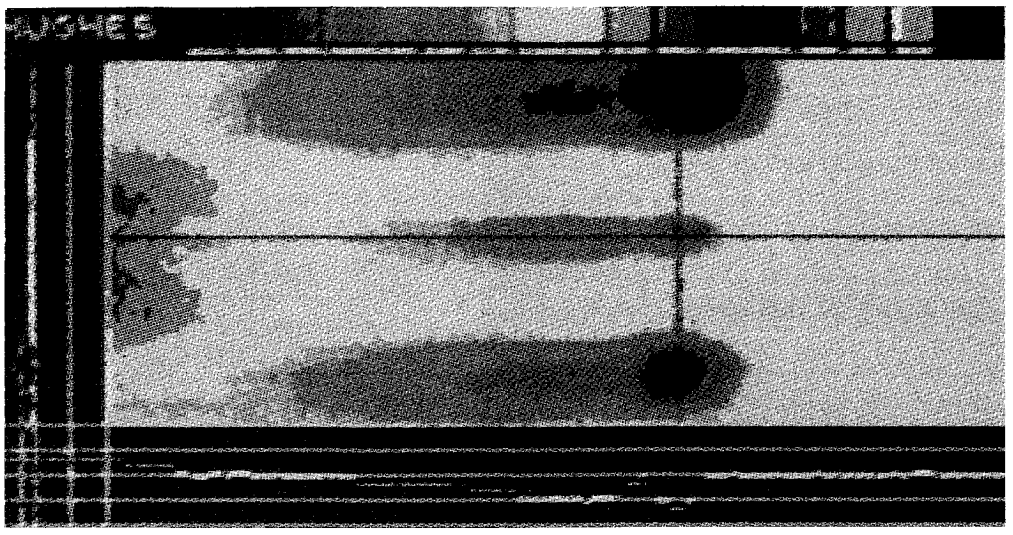

Fig. 9 Infrared thermograph of 2.8-, 0.7-, and 1.7-mm-high roughness elements in a turbulent boundary layer. Gray shades indicate temperature contours.

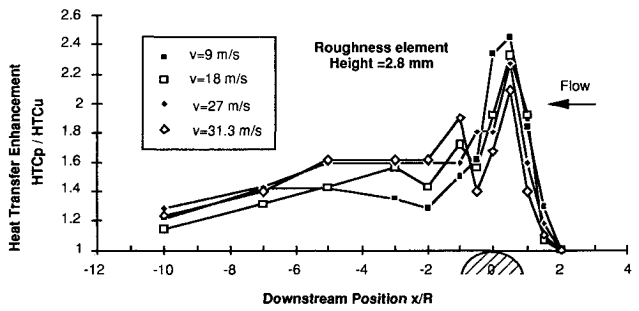

Fig. 10 Heat transfer coefficient enhancement profile on a 2.8-mm-high roughness element in a turbulent boundary layer.

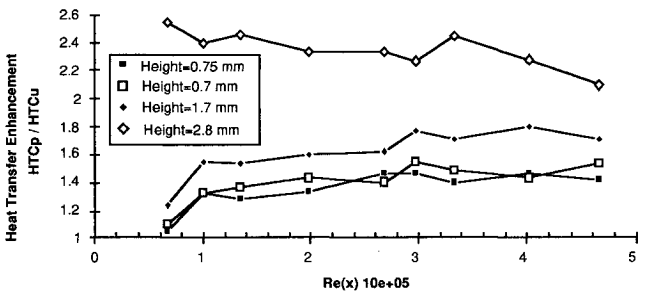

Fig. 11 Maximum heat transfer coefficient enhancement in a turbulent boundary layer vs Reynolds number.

transfer coefficient increases slowly, then increases strongly when the height of element roughness is the same order as the boundary-layer thickness. The roughly exponential increase of heat transfer with h/δ reflects the velocity profile above the plate. This indicates that the enhancement on the upstream face is due to the increased ventilation experienced by the roughness as it protrudes from the boundary layer.

C. Turbulent Boundary-Layer Results

1. Typical Infrared Image

A typical IR thermograph for a turbulent boundary-layer case at a freestream velocity of 18 m/s is shown in Fig. 9. The temperature is similar on each element, indicating that the heat transfer enhancement is less dependent on roughness size than for the laminar case. In addition, the enhanced heat transfer in the wake only persists a limited distance downstream of the element, unlike the transition wedges observed in the laminar cases.

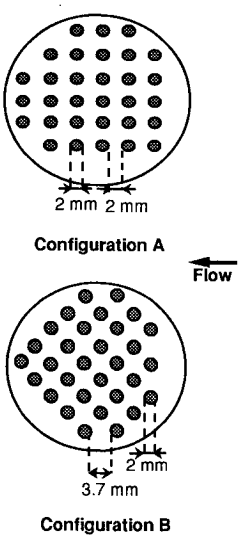

Fig. 12 Roughness test configurations A and B.

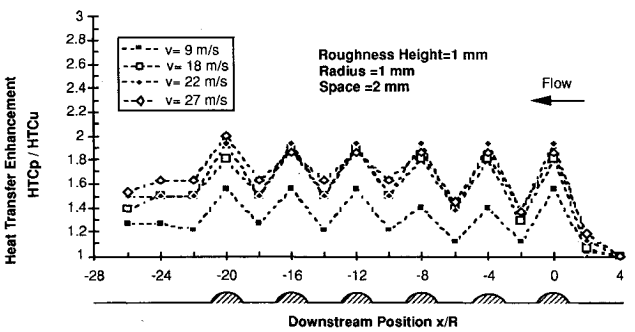

Fig. 13 Multiple roughness element heat transfer coefficient enhancement profile for configuration A.

2. Heat Transfer Enhancement Profiles

The heat transfer enhancement profiles observed for the 2.8-mm-high element in a turbulent boundary layer are shown in Fig. 10. The observed heat transfer enhancement profiles for the turbulent boundary layer are quite similar to those observed with a laminar boundary layer. However, the magnitude of the heat transfer enhancement is reduced due to the higher heat transfer in the unperturbed reference region. The ratio of heat transfer coefficient is seen to begin increasing approximately 1 diam upstream of the element until it reaches

a peak value of approximately 2.5. It then decreases to a minimum value at the downstream edge of the element. The heat transfer is seen to increase slightly at the upstream edge of the wake and then to decrease to a value between 20–50% of the unperturbed heat transfer.

3. Maximum Heat Transfer Enhancement on Elements

The maximum heat transfer enhancements observed for the turbulent boundary-layer cases are shown in Fig. 11 as a function of the local Reynolds number Re_x. The maximum heat transfer value extends from 1.5 for the small elements, to 2.5 for the 2.8-mm-tall roughness. The variation with Reynolds number is observed to be relatively weak. It should be noted that, because unperturbed heat transfer is high, the maximum heat transfer coefficients are actually higher than for laminar boundary-layer cases.

D. Multiple Roughness Element Effects

In order to study the influence of multiple roughness elements on heat transfer, the two configurations shown in Fig. 12 were tested under turbulent boundary-layer conditions. The multiple roughness configurations were constructed of 1-mm-high, 2-mm-diam wax bead elements. Configuration A consisted of a series of elements, spaced 2 mm apart in a rectangular grid. Configuration B used the same series of elements rotated by 45 deg, resulting in a staggered distribution with elements spaced 3.7 mm apart.

1. Heat Transfer Enhancement Profiles

The heat transfer coefficient profiles along the central row of elements are plotted as a function of the distance from the center of the first roughness element in Figs. 13 and 14. It should be noted that the IR thermographs were only sampled at the top of the elements, and at one or two points within the gaps. For configuration A, the profiles are quite similar, with the exception of the lowest velocity tested (9 m/s). The heat transfer coefficient enhancement is approximately 2 at the top of elements and 1.5 in the gaps. For configuration B, the profiles are similar for each velocity. The peak values are approximately the same as for configuration A, and a plateau in the heat transfer coefficient enhancement can be seen between each element.

For configuration B, values of heat transfer coefficient enhancement were compared to Stanton number obtained in a similar configuration by Hosni et al.,[3] who studied rough plates covered with staggered 1.27-mm-diam hemispherical elements with a 2-diam gap space. For a test velocity of 27 m/s, Hosni et al. found average Stanton numbers of approximately 0.004 in the rough zone, and 0.0025 in a smooth zone. Therefore, the ratio of observed Stanton number in the rough zone to the smooth zone corresponds to an average heat transfer enhancement of 1.6. This average value is consistent with the local heat transfer coefficient enhancements of 1.5 in the gap space and 2 on the top of element found in this study.

E. Effect of Roughness Element Separation

In order to study the effect of element separation, two roughness element arrangements were tested. Configurations C and D are shown in Fig. 15. Configuration C consisted of two regions. In the upper zone, the roughness elements were close packed to form a dense roughness zone. For comparison to configuration B, two rows of roughness elements were spaced 2 mm apart in the lower zone. Configuration D consisted of five regions of varying separation. The space between elements was 0.5, 1, 1.5, 2, and 0 mm (close pack).

1. Comparison of Heat Transfer Coefficient Profiles

Heat transfer coefficient enhancement profiles for the close pack zone in configuration C are presented in Fig. 16. The heat transfer is seen to be uniform along the rough zone and to vary with velocity from 1.3 to 1.6. In the downstream separation region, the heat transfer enhancement is minimal

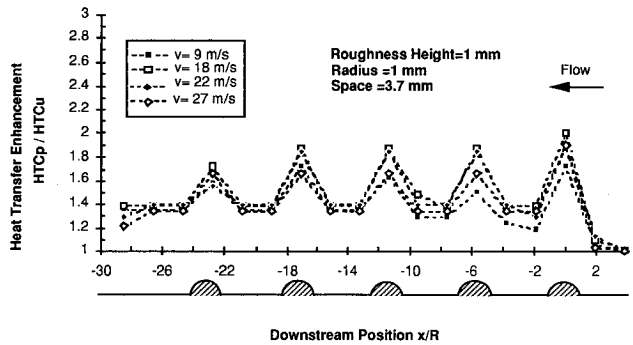

Fig. 14 Multiple roughness element heat transfer coefficient enhancement profile for configuration B.

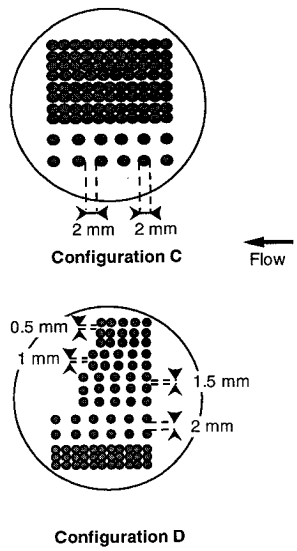

Fig. 15 Roughness test configurations C and D.

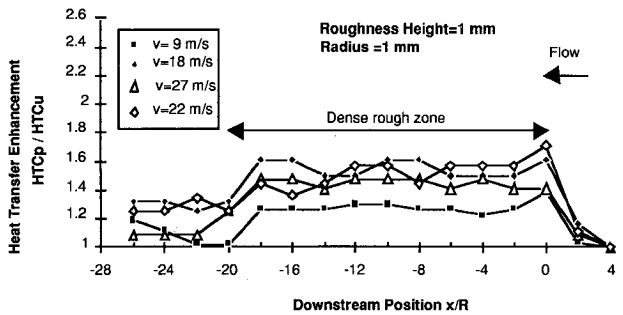

Fig. 16 Heat transfer coefficient enhancement profile in a dense rough zone for configuration C.

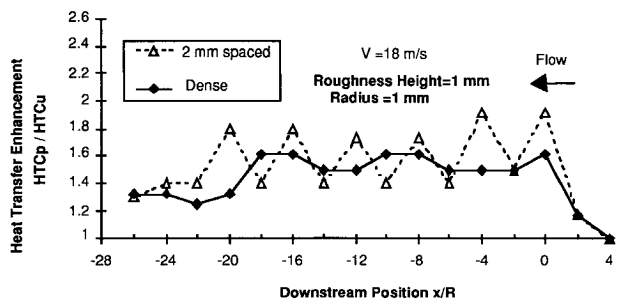

Fig. 17 Comparison between heat transfer coefficient enhancement with densely packed roughness elements and 2-mm spaced roughness elements.

for the 9 m/s case and slightly higher for other velocities. The observed heat transfer coefficient enhancement of 1.4 for the 27 m/s case is in a good agreement with the average Stanton number heat transfer enhancement of 1.6, calculated from experimental results obtained by Healzer et al.[11] on a fully rough porous plate.

In Fig. 17, heat transfer coefficient enhancement profiles in the dense and 2-mm separation zones from configuration C are compared, for a freestream velocity of 18 m/s. The heat transfer coefficient enhancement in the dense roughness zone is observed to be between the minimum and maximum values obtained for the spaced roughness elements regions.

Heat transfer coefficient enhancement profiles were also studied for all the roughness element spacings in configuration D. A distinct change in the behavior was observed between the 1–1.5-mm separation cases. At lower separation, the heat transfer enhancement was uniform with no indication of individual elements. At 1.5 mm and greater separations, the effect of individual elements was clearly evident in the heat transfer profiles.

VII. Conclusions

This investigation of the heat transfer variation on surface roughness elements has yielded the following observations and conclusions.

1) A noninvasive method, using IR techniques, has been developed that allows high spatial scale measurement of heat transfer variation on individual roughness elements.

2) Preliminary measurements were made on hemispherical roughness elements on a flat plate. Significant enhancement in heat transfer was observed on the roughness elements and in the wake when the elements protruded into the boundary layer. The highest heat transfer was observed on the upstream face of the elements.

3) For laminar boundary-layer conditions, the maximum heat transfer enhancement (referenced to the unperturbed flat plane) was observed to increase with roughness element size. Heat transfer enhancements as high as 8 were observed for elements whose height was 1.3 times the theoretical boundary-layer thickness. In addition, some enhancement in heat transfer was observed upstream of the element.

4) For turbulent boundary-layer conditions, the maximum heat transfer enhancement was not strongly dependent on velocity for the conditions tested. The peak heat transfer enhancements were observed to be between 2.1–2.6 times the unperturbed turbulent heat transfer for the flat plate.

5) The interaction of multiple roughness elements was studied for 1-mm-high elements under turbulent boundary-layer conditions. If the roughness elements were closely packed, the heat transfer was observed to be relatively uniform. However, for roughness element separation's greater than approximately 1 mm, the heat transfer on each element was observed to be similar to that observed for the individual elements.

6) The observed enhancement in heat transfer on individual roughness elements is consistent with proposed physical models for glaze ice accretion. The enhanced heat transfer on the upwind face of the roughness elements explains the enhanced growth into the flow observed for feather ice growth. The observed enhancement of approximately 2.5 in the turbulent boundary-layer case may be useful in predicting the onset of feather growth. The enhanced heat transfer observed upstream of the physical roughness element for the laminar boundary-layer conditions may explain the upstream propagation of the smooth-rough transition boundary observed for some glaze ice conditions.

Acknowledgments

This work was supported in part by La Direction des Recherches et Études Techniques, the National Aeronautics and Space Administration, and the Federal Aviation Administration under Grants 92/1436/A000/DRET/DR/SR, NAG-3-666, and NGL-22-0069-640, respectively. The work was also supported by the National Science Foundation Presidential Young Investigators Program, Award 8552702.

References

[1]Hansman, R. J., and Kirby, M. S., "Comparison of Wet and Dry Growth in Artificial and Flight Icing Conditions," *Journal of Thermophysics and Heat Transfer*, Vol. 1, No. 3, 1987.

[2]Hansman, R. J., Breuer, K. S., Hazan, D., Reehorst, A., and Vargas, M., "Close-up Analysis of Aircraft Ice Accretion," AIAA Paper 93-0029, Jan. 1993.

[3]Hosni, M. H., Coleman, H. W., and Taylor, R. P., "Measurements and Calculations of Rough-Wall Heat Transfer in the Turbulent Boundary Layer," *International Journal of Heat and Mass Transfer*, Vol. 34, No. 4/5, 1991, pp. 1067–1082.

[4]Rohsenhow, W. M., and Choi, H., *Heat, Mass, and Momentum Transfer*, Prentice-Hall, Englewood Cliffs, NJ, 1961, pp. 132–207.

[5]Beckwith, I. E., "Experimental Investigation of Heat Transfer and Pressure on a Swept Cylinder in the Vicinity of Its Intersection with a Wedge and Flate Plate at Mach Number 4.15 and High Reynolds Numbers," NASA TN D-2020, 1964.

[6]Bushnell, D. M., and Jones, R. A., "Heat Transfer to a 70 Deg Swept Fin Partly Submerged in a Turbulent Boundary Layer at Mach 6," NASA TM-X-1191, 1965.

[7]Bushnell, D. M., "Interference Heating on a Swept Cylinder in a Region of Intersection with a Wedge at Mach Number 8," NASA TN D-3094, 1965.

[8]Van Fossen, G. J., Simoneau, R. J., Olsen, W. A., and Shaw, R. J., "Heat Transfer Distributions Around Nominal Ice Accretion Shapes Formed on a Cylinder in the NASA Lewis Icing Research Tunnel," AIAA Paper 84-0017, Jan. 1984.

[9]Browand, F. K., "An Experimental Investigation of the Instability of an Incompressible Separated Shear Layer," *Journal of Fluid Mechanics*, Vol. 26, 1966, pp. 281–307.

[10]Schlichting, H., "Boundary Layer Theory," 7th ed., McGraw-Hill, New York, 1979.

[11]Healzer, J. M., Moffat, R. J., and Kays, W. M., "The Turbulent Boundary Layer on a Rough, Porous Plate: Experimental Heat Transfer with Uniform Blowing," Mechanical Engineering Dept., Stanford Univ., Report HMT-18, Stanford, CA, 1974.